Effect of Melt Temperature on Surface Films Formed on Molten AZ91D Alloy Protected by Graphite Powder

WEIHONG LI, JIXUE ZHOU, BAICHANG MA, JINWEI WANG, JIANHUA WU, and YUANSHENG YANG

Graphite powder was adopted to prevent AZ91D alloy from oxidizing during melting and casting. The microstructure of the resultant surface films, formed at 933 K, 973 K, 1013 K, and 1053 K (660 °C, 700 °C, 740 °C, and 780 °C) for 30 minutes, was investigated by scanning electron microscopy, energy dispersive spectrometer, and X-ray diffraction, and the phase composition of the surface films was analyzed by the standard Gibbs free energy change of the reactions between the graphite powder, the alloy melt, and the ambient atmosphere. The effect and mechanism of melt temperature on the resultant surface films were also discussed. The results indicated that the surface films, of which the surface morphology comprised folds and wrinkles, were composed of a protective layer and MgF_2 particles. The protective layer was contributive to the prevention of the molten alloy from oxidizing, and consisted of magnesium, oxygen, fluorine, carbon, and a small amount of aluminium existing in the form of MgO, MgF_2, C, and $MgAl_2O_4$. The layer thickness was 200 to 900 nm. The melt temperature may affect the surface films through the increased interaction between the graphite powder, the melt, and the ambient atmosphere. The oxygen content and thickness of the protective layer decreased and then increased, while the height of the folds increased with melt temperature.

DOI: 10.1007/s11663-017-1064-z

I. INTRODUCTION

MAGNESIUM alloys are widely used in many industry fields due to their excellent intrinsic properties, such as low density, high specific strength, and high specific rigidity. However, the oxidation of the magnesium during the melting process limits the alloy's application in industry. To combat the oxidation problem, certain protective methods are applied during the melting and casting process. Such methods include the addition of flux to the melt, protective gas, alloying with ignition-proof materials, and vacuum protection.[1,2]

In the early stage of oxidation prevention, fluxes were widely used for protecting the magnesium alloys due to exhibition of effective prevention and ease of application. However, fluxes release harmful gases at high temperatures, which will not only pose a serious threat to human health, but also corrode the equipment.[2] Recently, gases, such as SO_2,[3,4] SF_6,[5] HFC-134a,[6] and HFC125,[7,8] have been used to protect molten magnesium alloys. Unfortunately, gases cause environmental problems because they act as greenhouse gases when released into the atmosphere.[9,10] Regarding the alloying method, the addition of the alloying elements deteriorates the mechanical properties of the magnesium alloys significantly.[11] Vacuum protection has no harmful side effects to the environment but the process raises the production cost of magnesium. The goal therefore is to find a cost-effective environmentally friendly solution to prevent the magnesium oxidation issue.

CO_2, which is not toxic or corrosive and cheaper than SF_6 and SO_2, has a lower degree of green house effect than SF_6.[12] Research has shown that CO_2 can protect molten magnesium in different forms. Fruehling[13] claimed that an atmosphere of pure CO_2 gas could effectively protect the magnesium melt. Emami and Sohn[12] used CO_2/air mixture to protect molten magnesium from oxidation. Yang and Lin[14] used CO_2 snow

WEIHONG LI, JIANHUA WU, and JIXUE ZHOU are with the Shandong Key Laboratory for High Strength Lightweight Metallic Materials, Advanced Materials Institute, Shandong Academy of Sciences, Jinan, 250014, Shandong, China. Contact e-mail: liweihong5236@163.com BAICHANG MA and JINWEI WANG are with the Shandong Engineering Research Center for Lightweight Automobiles Magnesium Alloys, Advanced Materials Institute, Shandong Academy of Sciences, Jinan, 250014, Shandong, China. YUANSHENG YANG is with the Institute of Metal Research, Chinese Academy of Sciences, Shenyang, 110016, Liaoning, China.

Manuscript submitted December 15, 2016.
Article published online August 7, 2017.

Table I. Chemical Compositions of AZ91D Alloy (Weight Percent)

Al	Zn	Mn	Si	Fe	Cu	Ni	Mg
9.1	0.67	0.16	0.02	0.003	0.01	0.002	bal.

to develop a highly efficient method for protecting magnesium melts. Thus, past research has shown that CO_2 is effective in protecting the molten magnesium.

Graphite can react with oxygen to produce CO_2 rather than CO below 1273 K (1000 °C) for the lower activation energies of CO_2 desorption than those of CO desorption.[15,16] The produced CO_2 is expected to act as a barrier for protecting molten magnesium from oxidation. Due to the formed barrier, the graphite powder has potential for protecting the molten magnesium alloys from oxidation during melting and casting. Surface films formed on molten magnesium under the protection of CO_2 were composed of MgO and C. The produced carbon powder filled the interstices of MgO grains to make the surface films dense, preventing oxygen from reaching the surface of the molten magnesium.[12] Our previous results[17] showed that graphite powder could protect AZ91D melt and the protection ability was affected by melt temperature. However, the microstructure of the resultant surface films requires further investigation to understand the protection mechanism.

Surface films, formed statically or dynamically,[18–23] are the products of the reactions between molten alloys and a protective medium. For example, Al_2O_3, $MgAl_2O_4$, and MgO were the products of the oxidation of Al alloys containing 0.3 to 4.5 wt pct magnesium in an atmosphere with a very low oxygen partial pressure.[24] Another example was seen when an entrapped air bubble could react with the aluminium-calcium alloys to produce alumina and calcium aluminate.[25] The thermodynamic method to phase formation can indicate whether a reaction will occur. The reactions between graphite powder, the melt, and the ambient atmosphere, of which the products may be the phases of the surface films formed on the AZ91D melt protected by graphite powder, also requires further analysis.

Melt temperature is one of the important parameters that affect the formation of the surface films. With an increase in melt temperature, the oxidation rate of molten AZ91D alloy in HFC-134a/air increases.[26] Furthermore, when molten magnesium was protected by SF_6 in conjunction with dilute gas, the thickness as well as the size and quantity of MgF_2 particles also increases with melt temperature.[27] Therefore, the variation of the surface films with melt temperature also needs understanding.

The present work is aimed at understanding the protection mechanism of graphite powder for molten magnesium alloy to find an optimal melt temperature to be used in industry. Reactions between graphite powder, the melt, and the ambient atmosphere were analyzed using the thermodynamic method. Experiments were then carried out to study the effect of melt temperature on the surface films. The results are thought to provide the theoretical support for industrial application of graphite powder as a protective medium for magnesium alloy melts.

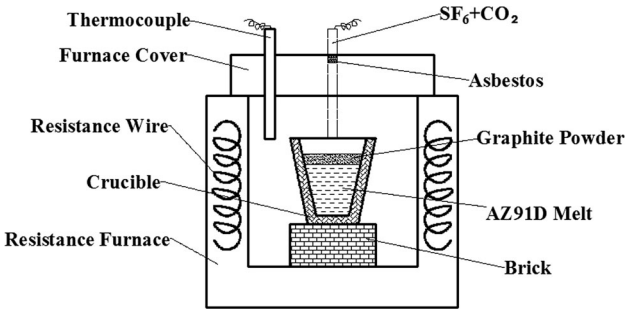

Fig. 1—Schematic diagram of the equipment used in this experiment.

II. EXPERIMENTATION

Commercial AZ91D alloy ingots were employed for the melting process. The chemical compositions are listed in Table I. The graphite powder was chemically pure with carbon content of no less than 99.85 wt pct, and its particle size was no more than 30 μm.

The ingots were melted in an electrical resistance furnace (Figure 1) and the surface films were thereby formed. The main components of the crucible were graphite and silicon carbide. Thermocouples were used to measure the furnace's atmospheric temperature. The furnace atmosphere temperature was assumed as the melt temperature.

The alloy, with the weight of approximately 500 g, and the crucible were placed inside of the furnace for the preheating process. Protective gas consisting of 99.5 vol pct CO_2 and 0.5 vol pct SF_6 was introduced when the temperature reached 673 K (400 °C). When the temperature stabilized at 973 K (700 °C), the protective gas pipe was removed and the molten alloy in the crucible was placed outside of the furnace. The old surface film of the melt was removed to expose the underneath melt. The newly exposed melt was protected by the gas for 1 minute and then 5.4 $g \cdot dm^{-2}$ graphite powder was uniformly distributed on the melt surface. Note that the newly exposed melt rapidly oxidized with cauliflower-like oxides appearing. Therefore, the gas continued to protect the fresh melt surface before the application of the graphite powder. Then, the melt was held at designed temperatures for 30 minutes to form surface films in the furnace with the hole for the protective gas pipe blocked by asbestos, and then air cooled outside of the furnace. Different surface films were formed at different temperatures. The melt temperature was designed to be 933 K, 973 K, 1013 K, and

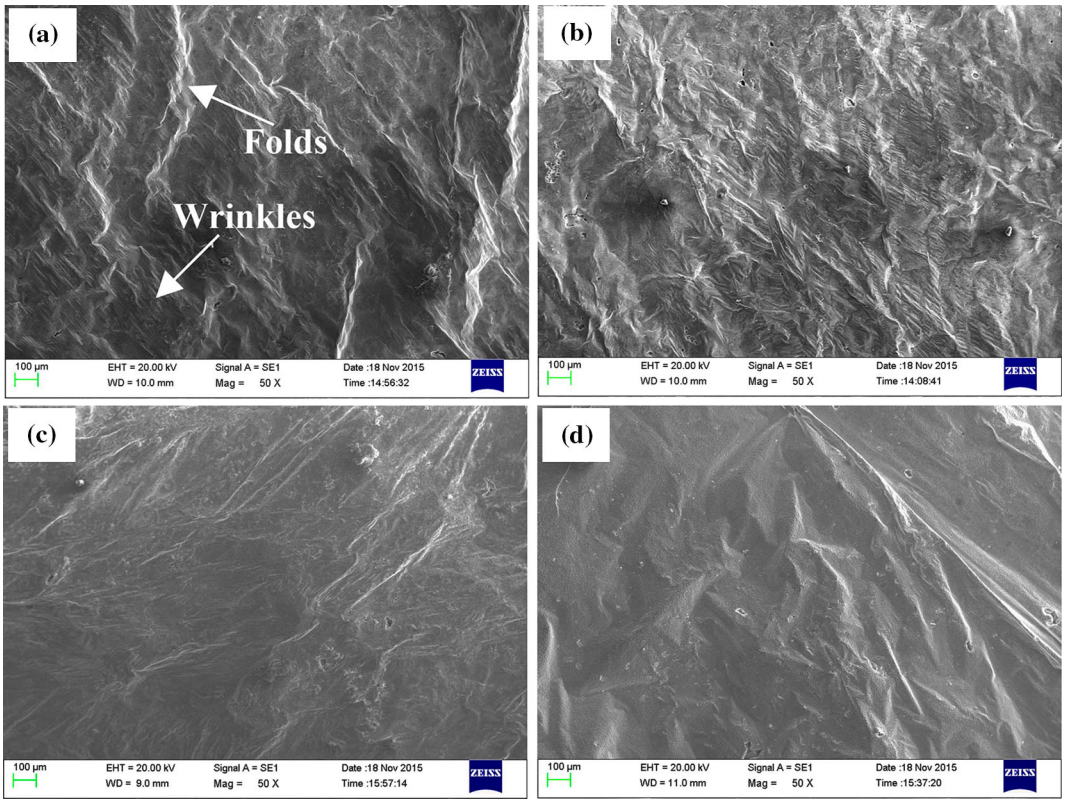

Fig. 2—Surface morphologies of the surface films formed at (*a*) 933 K (660 °C), (*b*) 973 K (700 °C), (*c*) 1013 K (740 °C), and (*d*) 1053 K (780 °C) for holding time of 30 min with 5.4 g·dm^{-2} graphite powder.

1053 K (660 °C, 700 °C, 740 °C, and 780 °C). The graphite powder was removed to observe the resultant surface films. No problem was encountered when removing the graphite powder from the AZ91D surface.

Two samples from each casting surface, with dimension of approximately 10 × 10 mm, were prepared. One was applied to observe the surface morphologies, and the other was applied for the cross-section sample. The cross-section sample was mounted, polished, and etched in 0.5 wt pct oxalic acid solution at room temperature for 15 seconds.

The surface and the cross-section morphology of the surface films were examined by EVO MA 10 scanning electron microscopy (SEM). Inca X-Max 50 energy dispersive spectroscopy (EDS) in conjunction with SEM was employed to analyze the elements. The phase composition of the surface films was determined using a D8 ADVANCE X-ray diffraction (XRD) with Mo Kα radiation. The samples for phase analysis by XRD were those used for surface morphology observation. All samples were ultrasonically cleaned before observation.

III. RESULTS AND DISCUSSION

A. *Effects of Melt Temperature on Surface Morphology of Surface Films*

Figure 2 presents the surface morphologies of the surface films formed at 933 K, 973 K, 1013 K, and 1053 K (660 °C, 700 °C, 740 °C, and 780 °C) for 30 minutes with 5.4 g·dm^{-2} graphite powder. The images reveal that the surface films are wrinkly. The wrinkly feature is classified into two categories, which are wrinkles and folds.[28] Wrinkles refers to the micro-sized features (Figure 2(a)), the formation of which was similar to those appearing on the dynamically formed surface films. The contraction coefficient is different between the surface film and the molten alloy, thus the wrinkles are postulated to be the result of the contraction stress exerted on the surface films.

Folds refer to the macro-sized features (Figure 2(a)), the formation of which was different from those that appeared on the dynamically formed surface films. Literature indicates that the formation of the folds was the result of turbulence of the molten alloy during casting.[28] However, the surface films in this work were formed under static conditions, thus the folds could not be the result of turbulence of the molten AZ91D alloy.

The formation of the folds may be relative to the solidification process. During solidification, solidified and molten AZ91D alloy could shrink at different proportions in volume. The melt had a larger volume shrinkage than the solid alloy. Some sites that solidified earlier became the peaks of the folds, while other sites that solidified later became the valleys.

The folds rather than the wrinkles, of which the height indicating the distance between the peak and the valley makes casting surfaces uneven, affect the surface quality. Therefore, the variation of the folds with melt temperature needs to be understood. When the melt

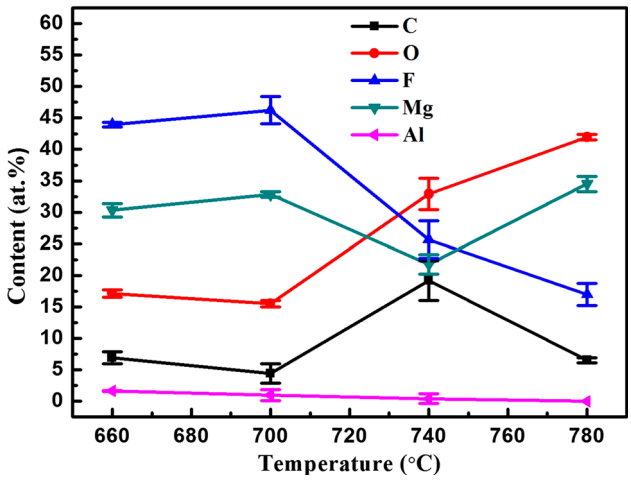

Fig. 3—Variation of the compositions of the surface films with melt temperature protected by 5.4 g·dm^{-2} graphite powder with holding time of 30 min.

temperature was 933 K (660 °C), the height of the folds was short (Figure 2(a)), which made the surface smooth. With the increase in melt temperature, the surfaces became uneven due to the increased height of the folds (Figures 2(b), (c)). When the melt temperature increased to 1053 K (780 °C), the surface was very uneven due to the further increased height.

The above results show that with the increase in melt temperature, the height of the folds increased, leading to the deterioration of the surface quality. Since everywhere on the melt surface may be different in the heat transfer condition, some sites at which the melt fast cooled and solidified may become the peaks of the folds. However, the temperature of the melt at the other sites remains high and may increase with melt temperature. According to Campbell,[29] the volume of the melt at high temperature decreases more greatly than that at low temperature. Therefore, the sites became the valleys with long distance from the peaks at high melt temperature.

B. *Effects of Melt Temperature on Compositions of Surface Films*

The compositions of the surface films formed at different melt temperatures were determined using EDS at an acceleration voltage of 5 kV. The composition determination was carried out at three different places with an area dimension of 2.301 × 1.732 mm on each surface film sample. The results show that compositions of the surface films mainly included fluorine, magnesium, carbon, oxygen, and a small amount of aluminium.

Figure 3 presents the variation of the chemical elements with melt temperature. With the increase in melt temperature, the oxygen content decreased and then increased, while the fluorine content increased and then decreased. The total content of oxygen and fluorine was approximately 60.1 at. pct. The carbon content of the surface films formed at 1013 K (740 °C) was as high as 19.2 at. pct, while that at other melt temperatures

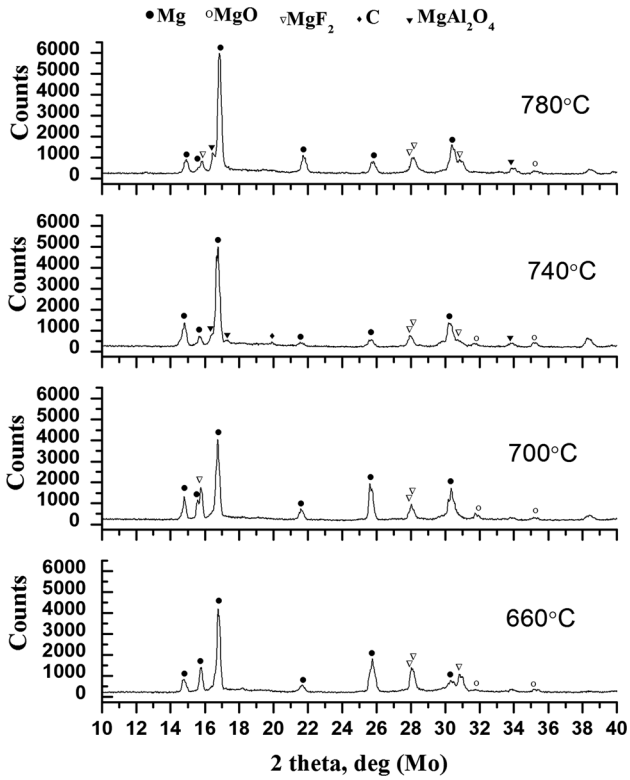

Fig. 4—XRD patterns of surface films formed at different temperatures for 30 min with 5.4 g·dm^{-2} graphite powder.

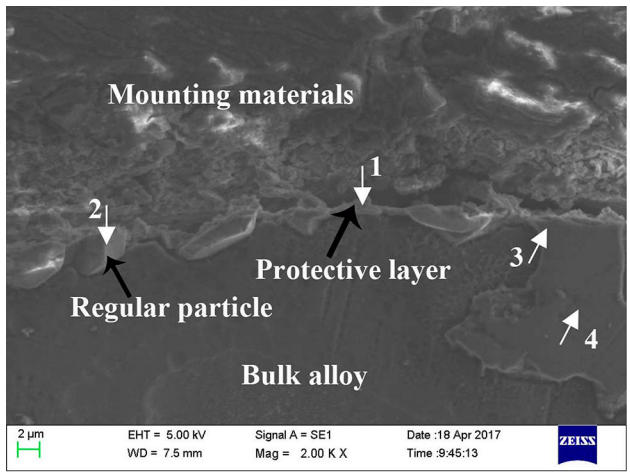

Fig. 5—Cross-section morphology of the surface film formed at melt temperature of 1013 K (740 °C) for 30 min with 5.4 g·dm^{-2} graphite powder.

was very low. The variation of the magnesium content with melt temperature was opposite to that of the carbon content, and the total content of the two chemical elements was approximately 39.1 at. pct.

The phase compositions of the surface films formed at different melt temperatures were analyzed by XRD, and the result is shown in Figure 4. Mg, MgO, and MgF_2 appeared at all melt temperatures. Obviously, Mg came from the bulk alloy. C appeared only at 1013 K (740 °C), while $MgAl_2O_4$ appeared at the melt temperature of 1013 K and 1053 K (740 °C and 780 °C).

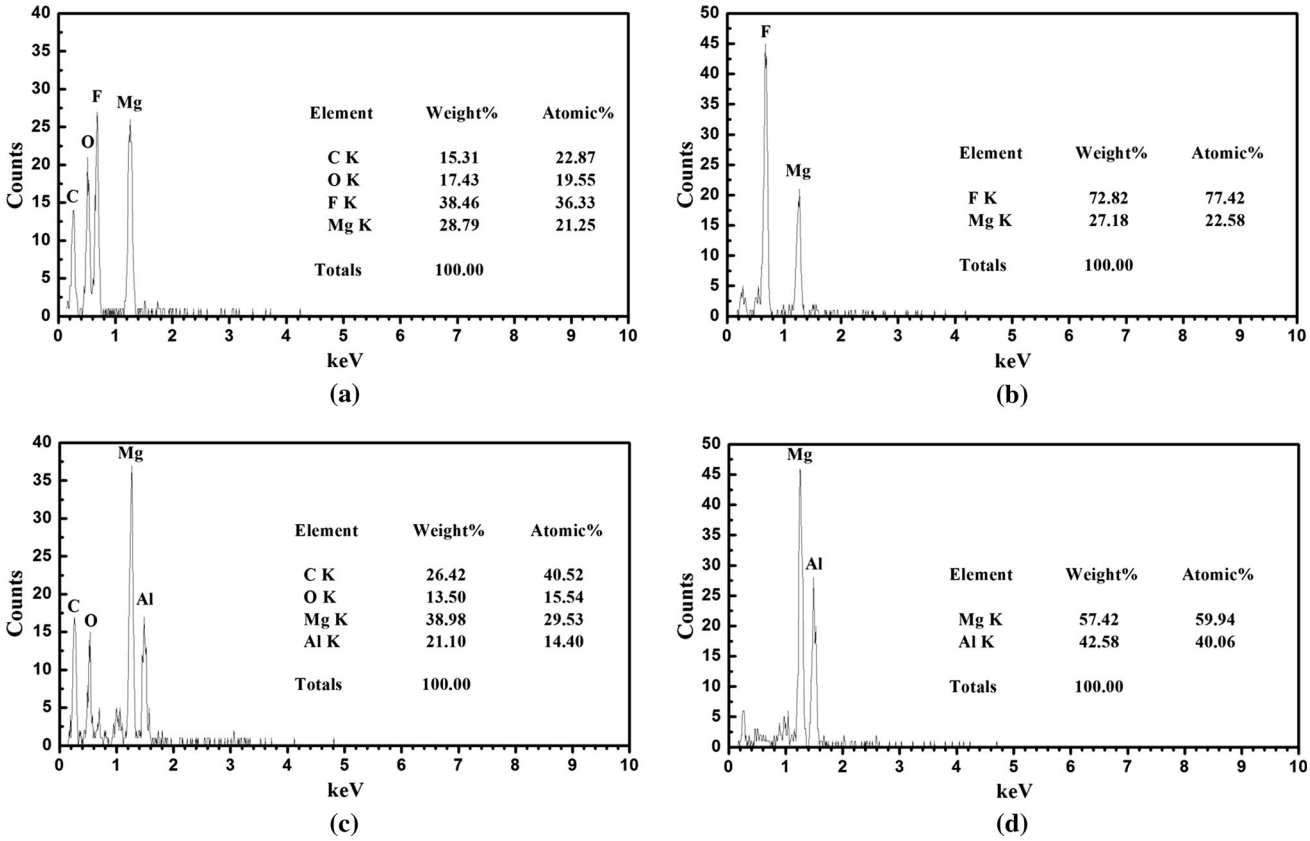

Fig. 6—EDS-spectra from cross-section morphology at Point 1 (*a*), Point 2 (*b*), Point 3 (*c*), and Point 4 (*d*) shown in Fig. 5.

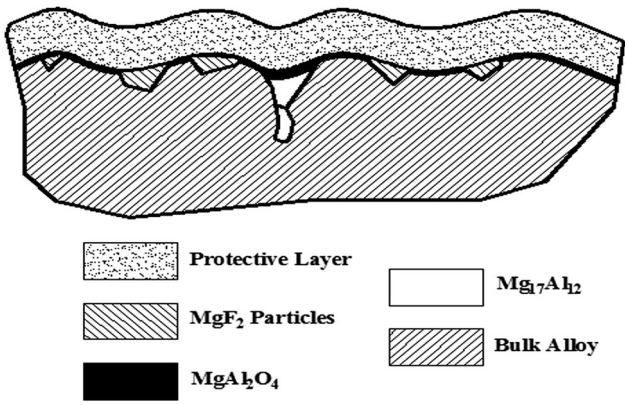

Fig. 7—Schematic illustration showing the structure of the surface film.

Reaction [1] shown below can readily occur due to the high affinity of magnesium to oxygen and the resultant MgO was an important phase of the surface films. However, MgO, with a Pilling–Bedworth ratio of 0.81 at 298 K (20 °C),[12] is porous and could not prevent the molten alloy from oxidation and volatilization.

$$\mathrm{Mg(l)} + \frac{1}{2}\mathrm{O_2(g)} = \mathrm{MgO(s)};$$

$$\Delta G^{\circ}_{993\ \mathrm{K}\ (720\ ^{\circ}\mathrm{C})} = -494.3\ \mathrm{kJ/mol}. \quad [1]$$

The graphite powder on the molten alloy surface can be removed easily and the surface film samples were ultrasonically cleaned before observation. Therefore, the phase of C detected by XRD (Figure 4) was not graphite powder but one phase of the surface films. The formation of the phase of C in surface films may be accomplished in two steps. First, graphite can react with oxygen in the atmosphere to produce carbon dioxide by the following chemical equation[16]:

$$\mathrm{C(s)} + \mathrm{O_2(g)} = \mathrm{CO_2(g)};$$

$$\Delta G^{\circ}_{993\ \mathrm{K}\ (273\ ^{\circ}\mathrm{C})} = -395.8\ \mathrm{kJ/mol}. \quad [2]$$

The oxidation of graphite belongs to the in-pore diffusion-controlled regime between 873 K and 1173 K (600°C and 900°C).[10] Second, the resultant carbon dioxide can continue to react with magnesium according to the following chemical reaction[12]:

$$\mathrm{2Mg(l)} + \mathrm{CO_2(g)} = \mathrm{C(s)} + \mathrm{2MgO(s)};$$

$$\Delta G^{\circ}_{993\ \mathrm{K}\ (720\ ^{\circ}\mathrm{C})} = -592.7\ \mathrm{kJ/mol}. \quad [3]$$

The MgO produced from Reaction [1] is highly porous and provides easy paths for CO_2 to react with Mg^{2+} ions diffusing from the molten alloy to the melt surface by Reaction [5]. The resulting carbon phase fills the interstices of MgO grains to form a protective layer of MgO–C.[12]

The generation of MgF_2 in the surface films may be relative to the SF_6 compound in the protective gas or the

residual fluorine in the melting furnace after the SF_6 supply was stopped.[30] SF_6 can react with Mg or MgO to produce MgF_2 as seen below[27,31–33]:

$$5Mg(l) + SF_6(g) + O_2(g) = 3MgF_2(s) + 2MgO(s) + \frac{1}{2}S_2(g);$$
$$\Delta G^{\circ}_{993K\,(720^{\circ}C)} = -2986 kJ/mol. \quad [4]$$

$$3MgO(s) + SF_6(g) = 3MgF_2(s) + SO_2(s) + \frac{1}{2}O_2(g);$$
$$\Delta G^{\circ}_{993K\,(720^{\circ}C)} = -803.6 kJ/mol. \quad [5]$$

MgF_2 (PBR = 1.29) covers the melt surface and increases the PBR of the surface films, acting as a barrier to further oxidation.[34]

$MgAl_2O_4$ are the product of gradual oxidation,[35] which may occur according to the following chemical reaction:

$$Mg(l) + 2Al(l) + 2O_2(g) = MgAl_2O_4(s);$$
$$\Delta G^{\circ}_{993\ K\ (720\ ^{\circ}C)} = -1883.0\ kJ/mol. \quad [6]$$

Aluminium is soluble in magnesium and can thus diffuse out to form $MgAl_2O_4$ at the interfacial layer between the oxide and the substrate, which may affect Mg diffusion from the substrate, preventing the melt from oxidizing.[36]

Based on the above analysis, the surface films formed on the molten AZ91D protected by graphite powder at different melt temperatures were the products of the reactions between the graphite powder, the melt, and the ambient atmosphere. The effects of melt temperature on the reactions resulted in the variation of the surface films in composition with melt temperature. However, how the melt temperature affects the reactions remain unknown that may be our future work. Our future works may also include to know the reason why the total content of oxygen and fluorine or that of magnesium and carbon of the surface films formed at different melt temperatures could be stable at 60.1 or 39.1 at. pct.

C. *Effects of Melt Temperature on Structure of Surface Films*

The cross sections were observed to understand the structure of the surface films formed at different melt temperatures. Figure 5 presents the observation result of the surface film formed at 1013 K (740 °C). The surface films were composed of a protective layer and regular particles. The protective layer was continuous and compact and was contributive to preventing the melt from oxidizing.

The chemical composition analysis of the surface film formed at 1013 K (740°C) was carried out using EDS to understand the distribution of the various phases. The results are given in Figure 6. The chemical compositions of the protective layer at Point 1 in Figure 5 consisted of F, C, Mg, and O (Figure 6(a)), and the phases were thought to be MgF_2, MgO, and C. The chemical

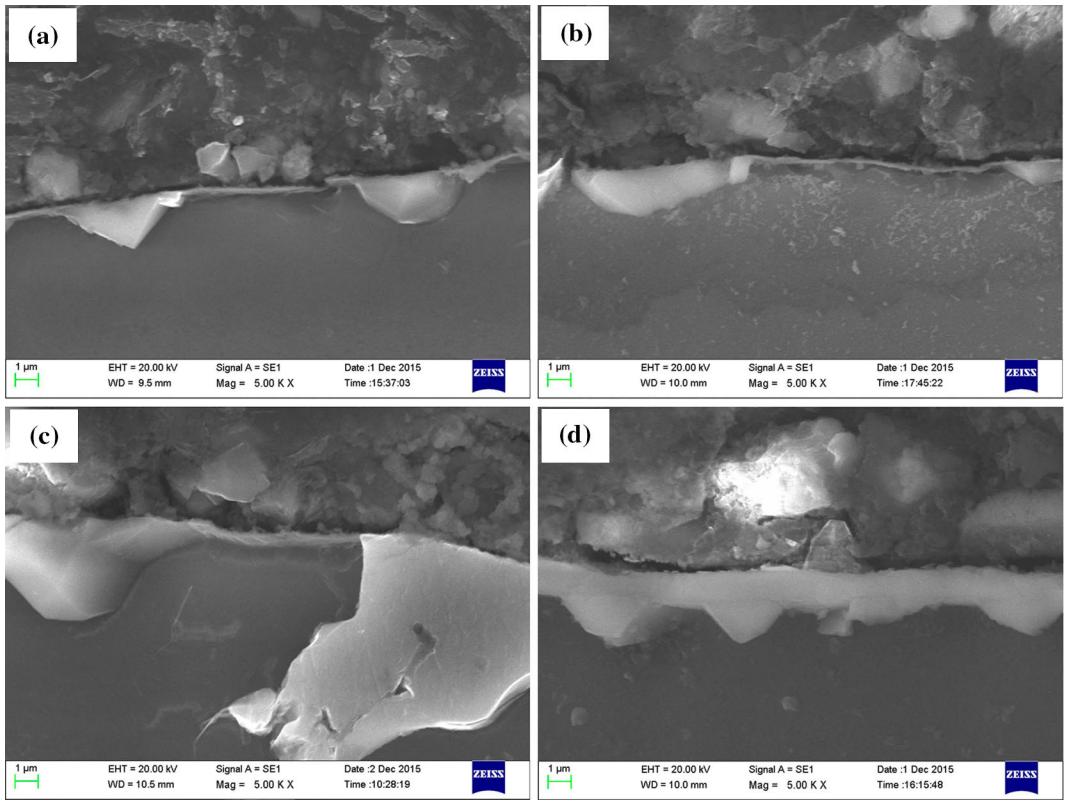

Fig. 8—Cross-section morphology at 5000× magnification of the surface films formed at (*a*) 933 K (660 °C), (*b*) 973 K (700 °C), (*c*) 1013 K (740 °C), and (*d*) 1053 K (780 °C) for holding time of 30 min with 5.4 g·dm^{-2} graphite powder.

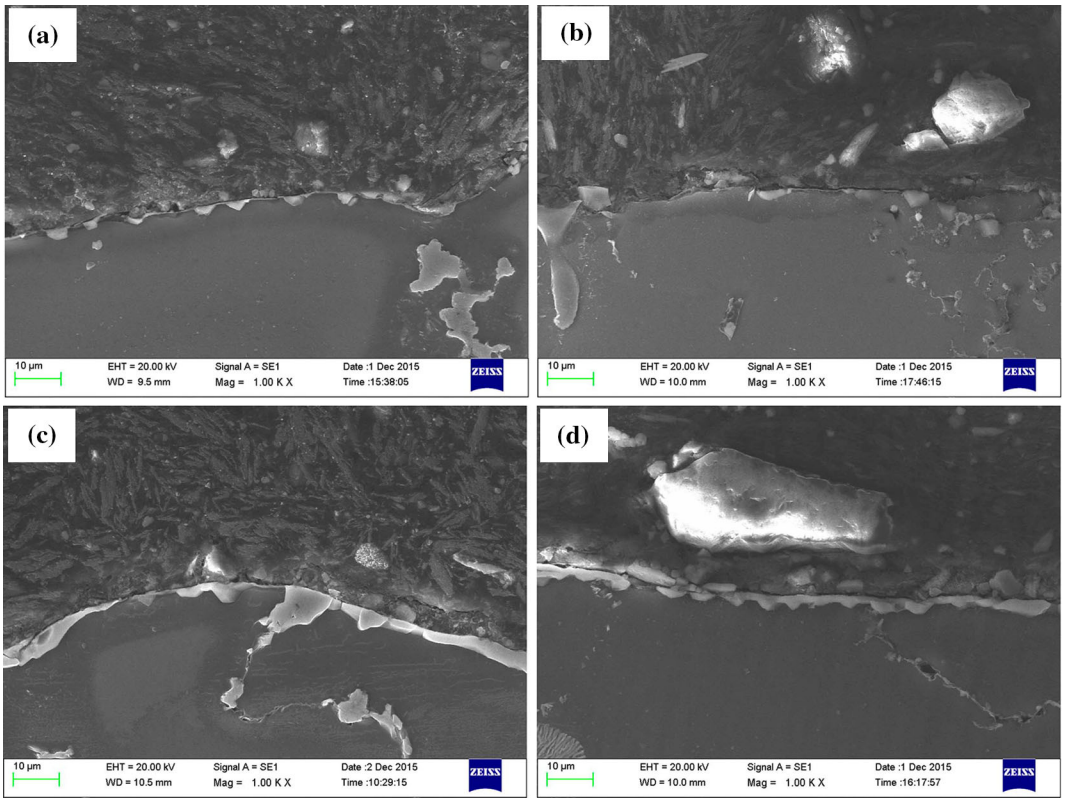

Fig. 9—Cross-section morphology at 1000× magnification of the surface films formed at (*a*) 933 K (660 °C), (*b*) 973 K (700 °C), (*c*) 1013 K (740 C), and (*d*) 1053 K (780 °C) for holding time of 30 min with 5.4 g·dm^{-2} graphite powder.

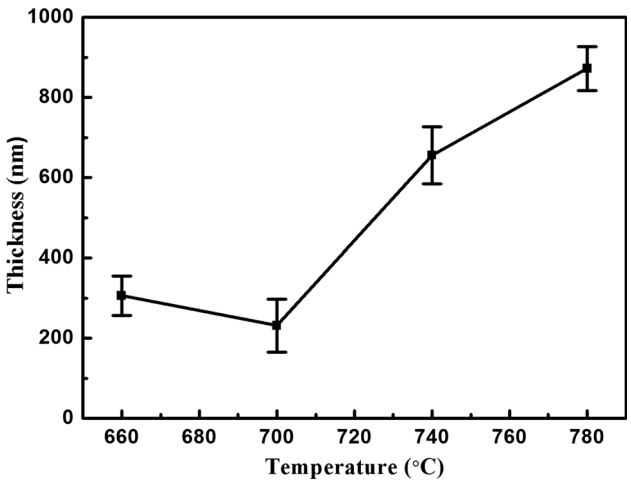

Fig. 10—Variation of the protective layers in thickness with melt temperature.

compositions of the regular particles at Point 2 (Figure 5) mainly consisted of F and Mg (Figure 6(b)), and the phase was thought to be MgF_2. The chemical compositions at Point 3 (Figure 5) consisted of C, Mg, O, and Al (Figure 6(a)), and the phases were thought to be $MgAl_2O_4$ and C.

An interesting phenomenon is found that F and Al did not exist simultaneously at the same place. Al frequently appeared at the interfacial layer between the protective layer and the phase of $Mg_{17}Al_{12}$ (as shown at Point 4 in Figures 5 and 6(d)), a common intermetallic compound phase in AZ91D,[37,38] and occasionally appeared at that between the protective layer and the bulk alloy. Therefore, the structure of the surface film may be schematically illustrated as shown in Figure 7.

The cross-section morphology of the surface films formed at different melt temperatures was observed with the results shown in Figures 8 and 9. The protective layer can be observed at high magnification (Figure 8), while the regular particles can be observed at relatively low magnification (Figure 9).

When the melt temperature was 933 K (660 °C), the protective layer was very thin and the thickness was approximately 306 nm (Figure 8(a)). The size of MgF_2 particles in the direction perpendicular to the protective layer was approximately 2 μm (Figure 9(a)).

When the melt temperature increased to 973 K (700 °C), the thickness of the protective layer decreased to approximately 232 nm (Figure 8(b)), while the size of the MgF_2 particles increased to approximately 3 μm (Figure 9(b)). The amount of MgF_2 particles also increased with the increase in melt temperature from 933 K to 973 K (660 °C to 700 °C).

When the melt temperature was 1013 K (740 °C), the thickness of the protective layer was increased greatly, and the amount of MgF_2 particles decreased greatly compared to those of the surface films formed at 933 K

and 973 K (660 °C and 700 °C). When the melt temperature increased to 1053 K (780 °C), the thickness of the protective layer increased to approximately 872 nm, and a large amount of MgF_2 particles with small size appeared.

The thickness range of the protective layers of the surface films formed at 933 K, 973 K, 1013 K, and 1053 K (660 °C, 700 °C, 740 °C, and 780 °C) was 200 to 900 nm. Figure 10 shows the variation of the protective layer in thickness with melt temperature. The thickness of the protective layer decreased first and then increased with the increase of the melt temperature.

The protective layers consisted of MgO, MgF_2, C, and $MgAl_2O_4$, which may be the products of the previously mentioned reactions. With increasing the melt temperature, the energy and then effective collisions of the reactant particles can increase, leading to the increase of the protective layers in thickness. However, when the melt temperature was at 973 K (700°C), the formation of MgF_2 particles may be dominant, resulting in the very low thickness of the protective layer.

IV. CONCLUSIONS

1. Surface films were prepared on molten AZ91D alloy protected by graphite powder at 933 K, 973 K, 1013 K, and 1053 K (660 °C, 700 °C, 740 °C, and 780 °C). The morphology of the surface films was wrinkly. The wrinkly morphology can be classified into folds and wrinkles. The height of the folds led to the surface unevenness, which was relative to the surface quality of castings. With the increase in melt temperature, the height of the folds increased, leading to the deterioration of castings in surface quality.
2. The compositions of the surface films consisted of magnesium, oxygen, fluorine, carbon, and a small amount of aluminium, existing in the form of MgO, MgF_2, C, and $MgAl_2O_4$. The variation of the oxygen content with melt temperature was opposite to that of fluorine, and that of magnesium was opposite to that of carbon. The oxygen content decreased and then increased with increasing the melt temperature.
3. The surface films were composed of a protective layer and MgF_2 particles. The protective layer, of which the thickness range was from 200 to 900 nm, is contributive to the effective prevention of the molten alloy from oxidizing. The thickness of the protective layer decreased first and then increased with the increase of the melt temperature. The melt temperature may affect the compositions, structure, and surface morphology of the surface films by affecting the reactions between the graphite powder, the AZ91D alloy melt, and the ambient atmosphere.

ACKNOWLEDGMENTS

Funding for this work was provided by the National Key Research and Development Program of China (No.2016YFB0701202 and No.2016YFB0301105). This work was also supported by the Natural Science Foundation of Shandong Province (No. ZR2016EMB11 and ZR2015YL007) and by the Youth Foundation of Shandong Academy of Sciences (No. 2014QN024). We greatly appreciate the help of Ian R. McAdams and Dr. Feng Gao for revising the English manuscript.

REFERENCES

1. V. Fournier, P. Marcus, and I. Olefjord: *Surf. Interface Anal.*, 2002, vol. 34, pp. 494–97.
2. A. Karger, F.W. Bach, and C. Pelz: *Mater. Sci. Forum*, 2005, vol. 488, pp. 85–88.
3. X.F. Wang and S.M. Xiong: *J. Mater. Sci. Technol.*, 2014, vol. 30, pp. 353–58.
4. X.F. Wang and S.M. Xiong: *Corros. Sci.*, 2013, vol. 66, pp. 300–07.
5. A. Mirak, C.J. Davidson, and J.A. Taylor: *Corros. Sci.*, 2010, vol. 52, pp. 1992–2000.
6. H.K. Chen and Z.F. Gong: *Trans. Nonferrous. Met. Soc.*, 2012, vol. 22, pp. 2898–05.
7. X. Zhang, G. You, J. Zha, and S. Long: *Rare Metal Mat. Eng.*, 2011, vol. 40, pp. 1496–99.
8. G.Q. You, S.Y. Long, and R.F. Li: *Mater. Sci. Forum*, 2007, vols. 546–549, pp. 119–22.
9. W. Ha, J.I. Youn, and Y.J. Kim: *Mater. Sci. Forum*, 2006, vols. 510–511, pp. 806–09.
10. H. Won, J.E. Lee, and Y.J. Kim: *Mater. Sci. Forum*, 2005, vols. 475–479, pp. 2543–46.
11. S.L. Cheng, G.C. Yang, J.F. Fan, Y.J. Li, and Y.H. Zhou: *Trans. Nonferrous. Met. Soc.*, 2009, vol. 19, pp. 299–04.
12. S. Emami and H.Y. Sohn: *Metall. Mater. Trans. B*, 2014, vol. 46B, pp. 226–34.
13. J.W.Fruehling: Ph.D. Thesis, University of Michgan, Ann Arbor, Michigan, 1970.
14. S.C. Yang and Y.C. Lin: *J. Clean. Prod.*, 2013, vol. 41, pp. 74–81.
15. C.I. Contescu, T. Guldan, P. Wang, and T.D. Burchell: *Carbon*, 2012, vol. 50, pp. 3354–66.
16. H. Badenhorst: *Chem. Eng. Sci.*, 2013, vol. 104, pp. 117–24.
17. W.H. Li, J.X. Zhou, B.C. Ma, J.H. Wu, J.W. Wang, H.H. Zhuang, Y.S. Yang, and X.H. Huang: *Mater. Sci. Forum*, 2017, vol. 898, pp. 111–17.
18. D. Dispinar and J. Campbell: *Int. J. Cast Met. Res.*, 2006, vol. 19, pp. 5–17.
19. J. Campbell and M. Tiryakioglu: *Aluminium Alloys* 2006*, Pts 1 and 2*, 2006, vol. 519–521, pp. 1453–60.
20. M. Divandari and J. Campbell: *Int. J. Cast Met. Res.*, 2005, vol. 18, pp. 187–92.
21. M. Divandari and J. Campbell: *Int. J. Cast Met. Res.*, 2004, vol. 17, pp. 182–87.
22. R. Raiszadeh and W.D. Griffiths: *Metall. Mater. Trans. B*, 2006, vol. 37B, pp. 865–71.
23. S.A. Azarmehr, M. Divandari, and H. Arabi: *Mater. Sci. Technol.*, 2012, vol. 28, pp. 1295–1300.
24. S. Amirinejhad, R. Raiszadeh, and H. Doostmohammadi: *J. Therm. Anal. Calorim.*, 2013, vol. 113, pp. 769–77.
25. B. Nayebi, A. Bahmani, M.S. Asl, A. Rasooli, M.G. Kakroudi, and M. Shokouhimehr: *J. Alloys Compd.*, 2016, vol. 655, pp. 433–41.
26. H. Chen: *Mater. Charact.*, 2010, vol. 61, pp. 894–98.
27. S.M. Xiong and X.L. Liu: *Metall. Mater. Trans. A*, 2007, vol. 38A, pp. 428–34.
28. A.R. Mirak, M. Divandari, S.M.A. Boutorabi, and J. Campbell: *Int. J. Cast Met. Res.*, 2007, vol. 20, pp. 215–20.
29. J. Compbell: *Castings*, 2nd ed., MPG Books Ltd., Bodmin, Cornwall, 2003, p. 205.
30. S.H. Nie, S.M. Xiong, and B.C. Liu: *Mater. Sci. Eng., A*, 2006, vol. 422, pp. 346–51.
31. S.H. Nie, S.M. Xiong, and Z. Liu: *Rare Metal Mat. Eng.*, 2007, vol. 36, pp. 21–25.

32. S.H. Nie, X.L. Liu, S.M. Xiong, and B.C. Liu: *J. Mater. Eng.*, 2005, vol. 6, pp. 3–6.
33. S. Emami, H.Y. Sohn, and H.G. Kim: *Metall. Mater. Trans. B*, 2014, vol. 45, pp. 1370–79.
34. W. Ha and Y.J. Kim: *J. Alloys Compd.*, 2006, vol. 422, pp. 208–13.
35. F. Czerwinski: *Acta Mater.*, 2002, vol. 50, pp. 2639–54.
36. T.S. Shih, J.B. Liu, and P.S. Wei: *Mater. Chem. Phys.*, 2007, vol. 104, pp. 497–04.
37. Y.J. Chen and P.S. Wei: *Mater. Trans.*, 2007, vol. 48, pp. 3181–89.
38. F. Czerwinski: *Corros. Sci.*, 2004, vol. 46, pp. 377–86.